

# Nanometer-Scale Layering in Rock Varnish: Implications for Genesis and Paleoenvironmental Interpretation<sup>1</sup>

David Krinsley, Ronald Dorn<sup>2</sup>, and N. K. Tovey<sup>3</sup>

Department of Geological Sciences, University of Oregon, Eugene, OR 97403-1272 USA

## ABSTRACT

Manganiferous rock varnish collected from Death Valley and Antarctica contains the smallest known terrestrial sedimentary deposits, with some layers only a few nanometers thick. Irregularities in these nanometer-scale layers are consistent with shrinking, cracking, and weathering of clay minerals. In the Death Valley rock varnish, very different High Resolution Transmission Electron Microscope (HRTEM) textures coexist that may be related to climatic change. HRTEM observations contradict previous microbial models of Mn-Fe enhancement, requiring a new three-step model of biomineralization and diagenesis for varnish formation.

## Introduction and Background

Rock varnish is a dark manganiferous coating on rocks in virtually every terrestrial weathering environment (Dorn and Oberlander 1982). Observations of sedimentary layering in rock varnish by Hobbs (1917) have been verified many times with light (Haberland 1975; Perry and Adams 1978) and scanning electron microscopy (Potter and Rossman 1977, 1979; Krinsley et al. 1990; Dragovich 1993), as well as geochemically (e.g., Hooke et al. 1969; Dragovich 1988; Dorn 1990, 1994). This layering is believed to be comprised of clastic clay minerals cemented by chemical deposits of manganese and iron oxides (Potter and Rossman 1977, 1979) where microbial-mediated precipitation of manganiferous oxides traps eolian clays (Dorn and Oberlander 1981, 1982; Krumbein and Jens 1981; Palmer et al. 1985; Jones 1991; Nagy et al. 1991; Staley et al. 1991; Raymond et al. 1992; Drake et al. 1993).

In this paper we present High Resolution Transmission Electron Microscope (HRTEM) imagery of never-before-seen nanometer-scale layering in rock varnishes from Death Valley and Antarctica, explore implications of HRTEM textures, calculate rates of formation of nanometer-scale layers in a

sample from Death Valley, and speculate on paleoenvironmental signals in HRTEM textures.

## Sampling Sites and Methods

The samples we examined appear macroscopically to be "classic" coatings of black rock varnish, yet they come from two very different environments. The Death Valley sample comes from a boulder on the Hanaupah Canyon alluvial fan, about 1.7 m above a sample of charcoal with a radiocarbon age of  $23,420 \pm 550$  B.P. (Beta 28805) (site identified in Dorn et al. 1989, p. 1367). The charcoal, collected directly underneath the uppermost debris-flow unit found at the surface, provides a maximum age for the onset of varnishing. The Antarctic varnish comes from the Texas Tech University collection, sampled from a slope of Mt. Van Valkenburg, Clark Mountains, Marie Byrd Land in Antarctica; no time information is available for the onset of varnishing. The chemistry of this sample is similar to other Mn-rich varnishes in Antarctica (Dorn et al. 1992).

Ultrathin sections were first prepared for observation with light and scanning electron microscopy (SEM), as well as for quantitative electron microprobe analysis. We obtained imagery on the same varnish at scales from  $500\times$  to  $500,000\times$  using lower resolution light, SEM, and lower magnification TEM imagery (e.g., figure 1a). Then, 3 mm discs were cut out of an uncovered, polished

<sup>1</sup>Manuscript received June 27, 1994; accepted October 3, 1994.

<sup>2</sup>Department of Geography, Arizona State University, Tempe, AZ 85287-0104, USA.

<sup>3</sup>School of Environmental Sciences, University of East Anglia, Norwich NR4 7TJ, UK.

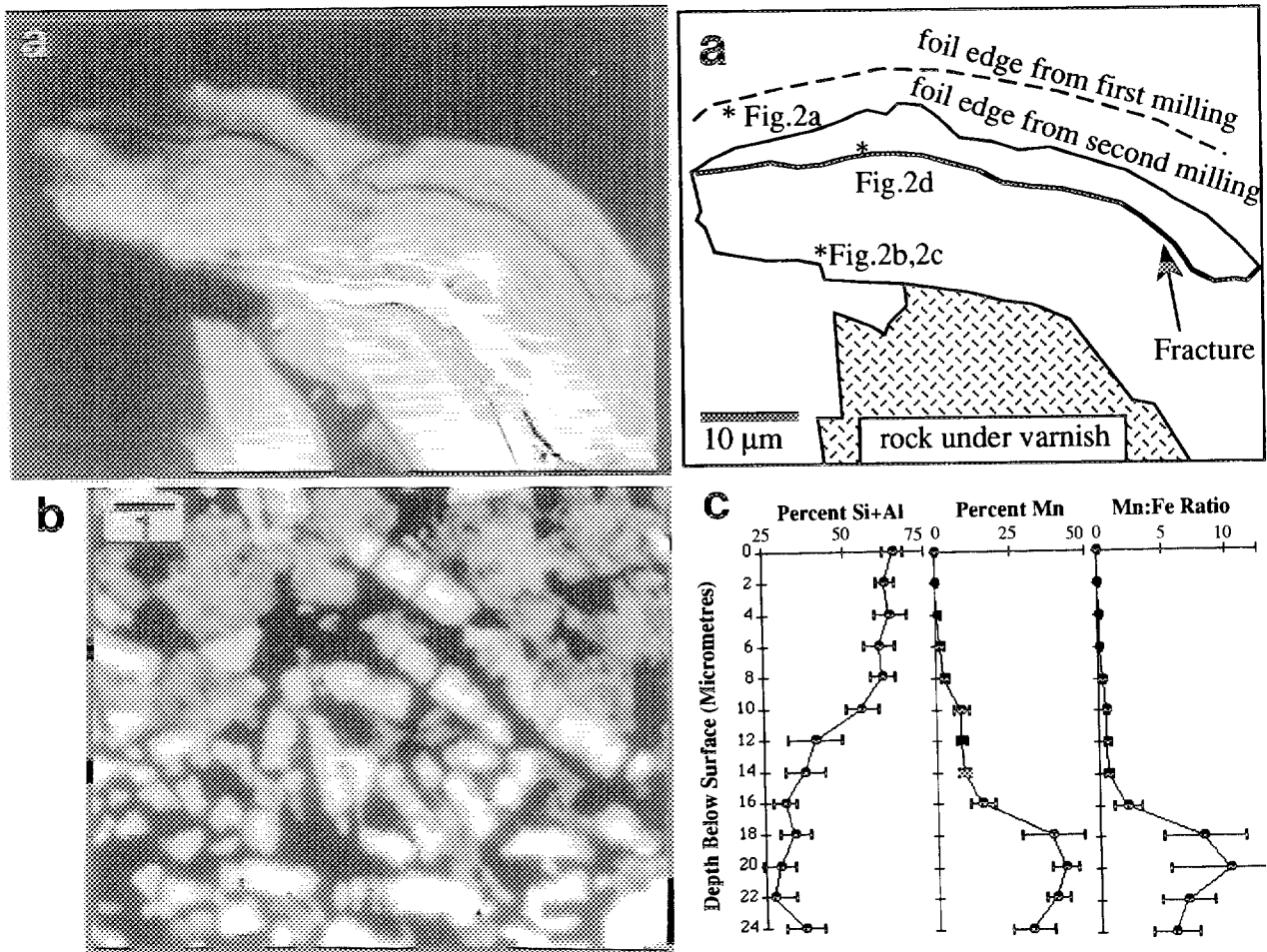


**Figure 1.** Backscatter electron microscope (BSE) and electron microprobe perspective on the sample from Hanaupah Canyon fan, Death Valley, California. *a.* BSE image of the ion-milled sample, and corresponding map showing the locations of HRTEM images (figure 2*a-d*). *b.* BSE image of the upper layer of varnish from this site that had been etched with HF, revealing bacterial clasts. This sample was collected from the same boulder as figure 1*a*, but ~5 cm away. Scale bar is 1 μm. *c.* Average and standard deviation of 15 wavelength dispersive electron microprobe transects (2 μm spot size; ZAF correction) from top to bottom. Thickness of the 15 varnish transects varied from 19–31 μm; depth was normalized by sampling 13 points evenly spread from top to bottom—and plotting them along the average depth of the transects of 24 μm.

thin section of rock varnish and placed on copper discs. After grinding the supporting glass, the sample was ion-thinned; this produces different degrees of sample transparency to the electron beam in bright-field TEM images (McLaren 1991).

### Results

Previous light, SEM, and electron microprobe tests have shown that Death Valley varnish has a manganese-poor upper layer and an underlying layer that is manganese-rich (Dorn 1988, 1994). Figure 1*b* illustrates oxide encrustations on rod-shaped bacteria that are commonly found only in the up-

permost few microns of this varnish. Focused beam (2 μm exciting X-rays up to 5 μm distant) wavelength dispersive electron microprobe measurements on 30 different bacterial casts yields Mn:Fe ratios that ranged between 0.01–1.20 with an average  $\pm 1$  S.D. of  $0.42 \pm 0.033$ , results similar to microprobe analyses in the upper layer of varnish from this site (figure 1*c*).

HRTEM imagery of the upper (Mn-poor) layer reveals a porous structure, with larger clay minerals that appear to be randomly distributed and oriented (figure 2*a*). Oval-shaped clays have typical lengths about 600 nm (range 100 to 1000 nm) with length:width ratios of about 0.3 (range 0.1 to 0.5).

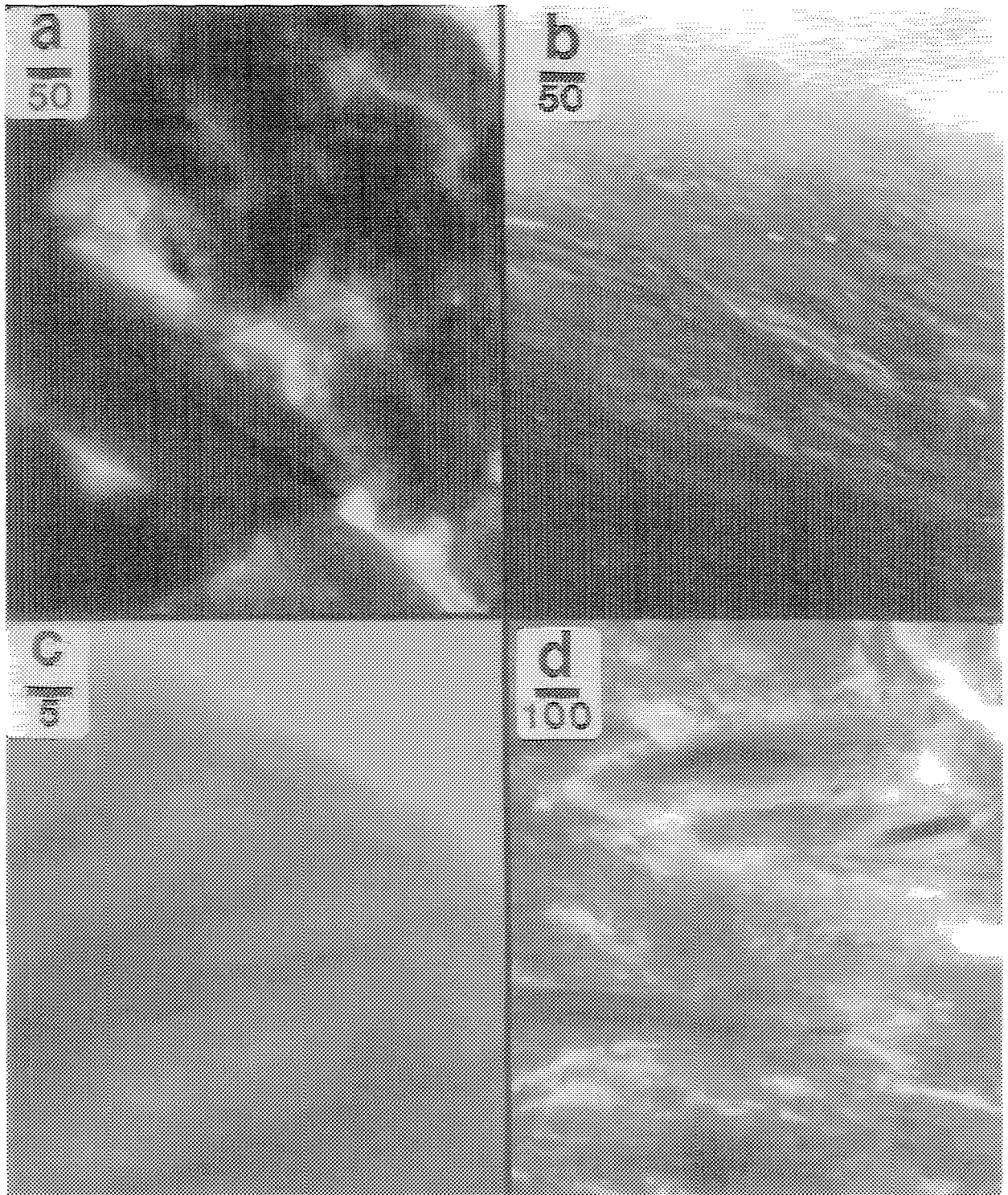


**Figure 2.** HRTEM images showing variations in electron transparency of the Death Valley sample. Scale bar in nanometers. *a.* The upper (Mn-poor) layer, where the largest elongated object extending upper right to lower left is probably montmorillonite. Round objects scattered throughout may be bacterial remnants or Fe-oxides. *b* and *c.* The lower (Mn-rich) varnish, where layers thicken and thin laterally indicating the space-transgressive nature of varnish accretion. The bottom half of *b* is dark because it is too thick to be electron transparent, and the upper right portion of *c* shows an amorphous layer created by electron beam bombardment. *d.* Transition between the upper and lower varnish, showing crude layering created by the subparallel orientation of the elongated clay minerals (probably montmorillonite).

These pods include illite and smectite, both of which are constituents of varnish identified by infrared analysis (Potter and Rossman 1977). Opaque spheres (~5 to 100 nm diameter) are common between the clay pods, which appear similar to hematite grains noted by Raymond et al. (1992, p. 329). Energy dispersive (EDS) analyses during HRTEM imaging reflect previous quantitative electron microprobe analyses (figure 1c): the major constituents of the upper layer are two-thirds  $\text{Al}_2\text{O}_3$  and  $\text{SiO}_2$  (ratio ~0.7) with about one-fifth  $\text{Fe}_2\text{O}_3$  and very low Mn:Fe ratios (<0.2). Minor components include Mg, K, Ca, P, and Ti. These measurements are consistent with infrared analysis of Mn-poor varnishes (Potter and Rossman 1977, 1979).

In the Mn-rich bottom part of the section, HRTEM imagery reveals a finely layered structure (figure 2b, 2c). Splitting of clays into monolayers (~2 nm thick) can be seen along with laminae as thick as 25 nm. Many minerals thicken and thin parallel with the layering, or wrap around larger minerals, while breakage and displacement of individual minerals occurs—disruptions that could be from wetting and drying, and clay weathering (Robert and Tessier 1992). Dark spots 1–10 nm in diameter are probably unit cells of Mn or Fe oxyhydroxides more resistant to ion milling. EDS analyses taken during HRTEM imaging are similar to quantitative electron microprobe data from the lowest layer (figure 1c): more than 40% Mn with very high Mn:Fe ratios (>5); less than one-third Al and Si (Al:Si ratios ~0.8). Minor components include Mg, K, Ca, and Ti.

The Antarctic sample contains only HRTEM-layered textures throughout the entire ~100  $\mu\text{m}$ -thick varnish (figure 3). Electron microprobe analyses reveal that Mn varies greatly from place to place, but typical values run between ~10–40%. Concentrations of Fe consistently average ~10% throughout the section. Individual layers varied from ~2 nm to >25 nm, and averaged ~8–14 nm in thickness over different images (figure 3a, 3b).

Throughout the Antarctic and Death Valley samples we observed microdivision phenomena (cf. Robert and Tessier 1992) where the clays divide to produce very small particles. We speculate the feathering to ~2 nm thick monolayers may be associated with the precipitation of Mn-Fe oxyhydroxide unit cells (e.g., figure 3b, 3c). It is also possible that some layering occurs by remobilization of oxides and subsequent evaporation of ultrathin liquid films (cf. Forcada and Mate 1993).

We observed features that are probably bacterial casts. First, their size and shape are appropriate for

bacteria, albeit smaller by a factor of 2–3 than those cultured (e.g., Dorn and Oberlander 1981, 1982; Palmer et al. 1985; Drake et al. 1993); the reduction may relate to desiccation. Second, the bright rims in backscatter images are from encrustations of Fe in figure 1b, and Mn in figure 3d—similar to encrustations on bacteria observed in other biomineralization systems (Ferris et al. 1987).

## Discussion

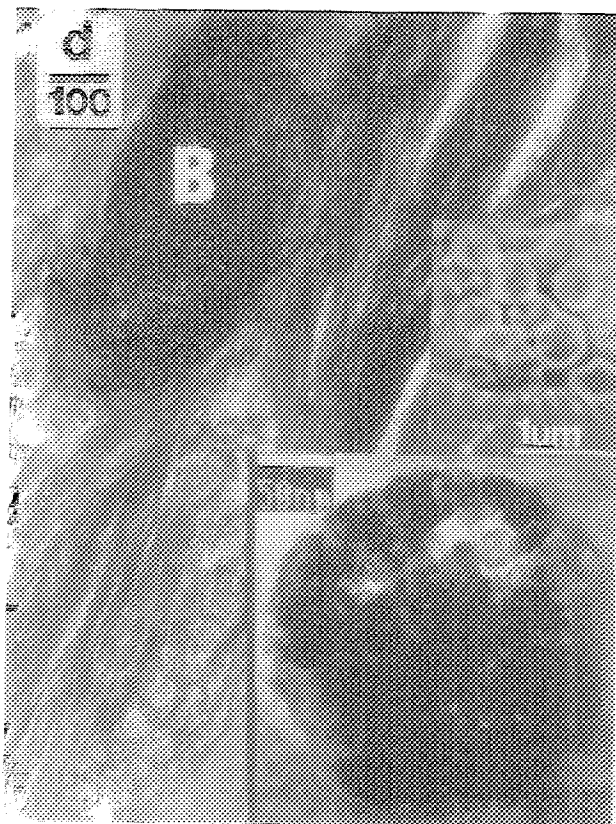
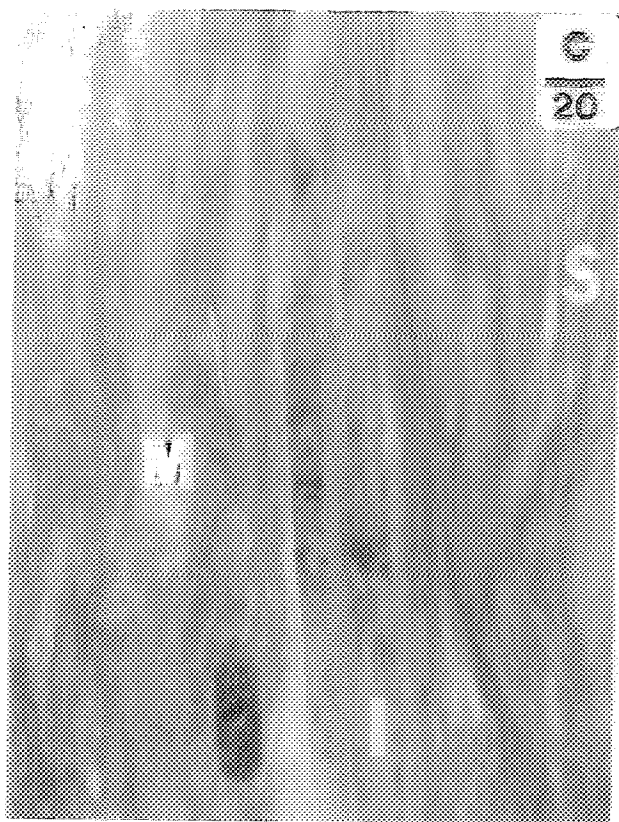
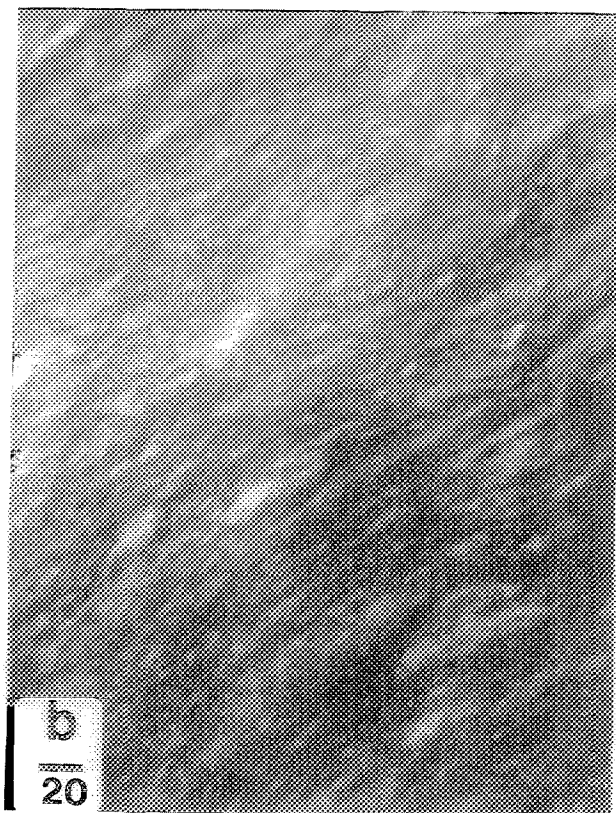
Sedimentary layers  $10^0$  to  $10^{-6}$  m thick are described commonly in aquatic and terrestrial settings (Boggs 1992; Krinsley et al. 1993). Sedimentary deposits have been reported at the nanometer-scale only for a few aquatic sequences, in particular for shales (Bennett et al. 1991). Rock varnish is the first known terrestrial sedimentary deposit displaying layering at the scale of  $10^{-9}$  m.

Nanometer-scale layering occurs in vastly different environments (figures 2, 3), although only the layered texture occurred in the Antarctic sample. Death Valley is a hot, subtropical desert where potential evapotranspiration greatly exceeds actual evapotranspiration. Antarctica is a cold desert with a limited set of terrestrial life forms (Friedmann 1993). Clearly, processes that develop nanometer-scale layering are not a simple function of gross tropospheric climate.

The paucity of microbial Fe-Mn casts or fragments of casts has been previously noted at light microscope and SEM magnifications (Dorn and Oberlander 1982). We previously speculated that sub-micron-sized bright lineaments seen in backscatter imagery might be oxide-encrusted bacterial remains (Krinsley et al. 1990; Krinsley and Dorn 1991). We therefore anticipated finding fragments of hydroxide-encrusted cell walls cementing clays at HRTEM magnifications. But layered varnishes from both Death Valley and Antarctica are composed of substantial quantities of Mn and Fe, with different layers containing 20 to >50% of Mn and Fe, and microbial remains can only account for a tiny fraction of the mass of Mn-Fe in varnish.

The disseminated nature of the vast majority of Mn-Fe hydroxides in nanometer-scale layered varnishes indicates that current simplistic models based on the biotic accumulation of Mn and Fe must be revised. If microorganisms are involved in the initial accumulation of Mn-Fe, as many argue (Krumbein and Jens 1981; Dorn and Oberlander 1981, 1982; Palmer et al. 1985; Jones 1991; Staley et al. 1991; Nagy et al. 1991; Raymond et al. 1992; Drake et al. 1993; Dorn and Meek 1995), we sug-





gest that there is a three-step model of varnish genesis involving biomineralization and diagenesis. Step 1 is the initial concentration of oxides in a cell cast (figure 1*b*, 3*d*). Step 2 is the remobilization of Mn-Fe from encrustations, as seen in historic varnishes (Dorn and Meek 1995). Step 3 is reprecipitation of the nanometer-scale oxides or hydroxides, perhaps through forming nanoaggregates (Robert and Tessier 1992) or the evaporation of ultrathin liquid film (cf. Forcada and Mate 1993). This conceptual model is consistent with our HRTEM results, but further tests of this model are required, including laboratory culturing and replication, and in situ observations of step 2 from different environments.

One alternative is an abiotic origin for Mn-enhancement involving Eh-pH fluctuations (cf. Smith and Whalley 1988). However, several aspects of rock varnish are inconsistent with an abiotic mechanism of Mn-enhancement: (1) The pH conditions on manganese-rich varnishes in deserts are near neutral (Dorn 1990) and not high enough to oxidize manganese by inorganic processes (Stumm and Morgan 1981). (2) Rock surfaces next to organisms that can change local pH conditions, such as lichens, often lack varnish. (3) Physiochemical fixation of Mn by clay minerals (El-Demerdashe et al. 1982) does not produce the concentrations of Mn found in varnish. (4) The patchy distribution of rock varnish is suggestive of biological colonization, while a chemical process would yield a more uniform deposit. Concomitantly, varnishes are slow to develop on smooth substrates like quartz, where microbial colonization is slowed but physiochemical mechanisms would not be inhibited. (5) Rock varnish is present in acidic environments that do not experience fluctuations in pH-Eh of sufficient magnitude to oxidize Mn (e.g., Dorn and Oberlander 1982; Douglas 1987). (6) Organic carbon is common within rock varnish (Dorn and DeNiro 1985). (7) The frequency of manganese-rich varnishes decreases in hyper-arid/hyper-alkaline regions (Jones 1991). This is

compatible with the inhibition of Mn-bacteria by alkalinity (e.g., Uren and Leeper 1978). (8) Varnish grows rapidly in periglacial and riverine environments that do not have sufficient alkalinity or high enough pH values to oxidize Mn, but there is a slow rate of varnish growth in deserts that do experience these fluctuations (see references on this topic in Dorn 1989, p. 168). This is predicted by a biotic model (Dorn and Oberlander 1982), but the opposite would be predicted by an abiotic model. (9) No laboratory experiment has yet produced Mn-rich varnish with Eh-pH fluctuations, while a field-based experiment showed that Mn-rich varnish could not be produced abiotically (Jones 1991).

Lastly, we speculate on possible paleoenvironmental signals for the textural change in the Death Valley sample. The very distinct chemical and textural change from the upper section (figure 2*a*, 1*c*) to the lower (figure 2*b*, 1*c*) layer is consistent with available evidence of climatic change in Death Valley, California. The observed relation between the moist/dry climatic change in Death Valley and chaotic/layered HRTEM texture in the Death Valley sample suggests that rates and styles of varnish accretion are influenced by environmental changes. In the latest Pleistocene from before 24,000  $^{14}\text{C}$  yr B.P. to  $\sim 10,000$   $^{14}\text{C}$  yr B.P., paleolake Manly was present in Death Valley (Hooke 1972; Dorn 1988), the vegetation varied from dwarf conifer woodland to Yucca-semidesert (Wells and Woodcock 1985), and groundwater recharge occurred in the region (Claassen 1986). In contrast, the last 10,000  $^{14}\text{C}$  yrs have been much more arid with desert scrub vegetation, dry alkaline lake beds, and abundant dust transport.

The greater abundance of dust matches the larger clay minerals in figure 2*a*, and greater alkalinity is known to produce the lower concentration of manganese (Dorn 1990; Jones 1991) found in the upper varnish layer (figure 1*c*). By comparison, a more positive water balance produced a lake, greater vegetation cover, and probably the finely layered varnish texture (figure 2*b*) greatly enriched

**Figure 3.** HRTEM images of variability in electron transparency of rock varnish from Mt. Van Valkenburg, Marie Byrd Land, Antarctica. Scale bar in nanometers. *a*. At a scale similar to figure 2*b*, the general consistency of layering is evident. The thickness through this section averages  $14 \pm 11$  nm. *b*. The reduction in layer thickness in this image ( $8 \pm 6$  nm) appears to correspond with clays weathering and the development of monolayers. *c*. In a higher magnification view, the mixed-layered illite-smectite clay minerals identified by Potter and Rossman (1977, 1979) can be seen in a continuum of soil clay organization where illitic clays with closed 1.0 nm layers (see area I) occur adjacent to interstratified clays (see area S). As clays undergo exfoliation and layer separation, monolayers form (see area M). *d*. Different views of likely bacterial casts. In the largest image, Mn-oxide crystals are found on the surface of the cast (B), as indicated by a very strong Mn-K $\alpha$  lines in EDS analysis of the area. In the larger inset image, Fe-K $\alpha$  lines are most intense. The smallest inset is a BSE image of bacteria in this section, resting on a feldspar detrital grain; the brighter rims are from higher Mn-concentrations.

in manganese (figure 1c). There is also a transition zone between these two extremes, perhaps reflecting climatic desiccation, where there are components of disorganization and layering (figure 2d).

### Conclusions

We use here HRTEM to produce new information concerning the structure and origin of rock varnish, and suggest that HRTEM may also be applied to the examination of other rock coatings. We present the first HRTEM images of nanometer-scale layering in rock varnish. Although we have only examined single samples of rock varnish from Death Valley and Antarctica, the disseminated nature of the manganiferous oxyhydroxides implies that current models of microbial Mn-Fe bioaccumulation must be revised. If microorganisms bioaccumulate Mn and Fe in rock varnish, we suggest that a three step process must occur:

(1) microbial concentration; (2) mobilization of Mn-Fe from microbes; (3) reprecipitation in a disseminated form in nanometer-scale layers. Although speculative, we note that the 24,000 yr-old Death Valley varnish records two dissimilar HRTEM textures that may have been caused by the major climatic change at about 10,000  $^{14}\text{C}$  yrs before present.

### ACKNOWLEDGMENTS

Supported in part by the State of Nevada, Nuclear Waste Project Office, and by Nye County, Nevada under a grant from the Nuclear Waste Fund (Krinsley), and in part by NSF Grant 8918644 (Dorn). We wish to acknowledge assistance from Alan Overson for technical assistance, and Dr. Maury Morgenstein, Geosciences Management Institute through Mifflin and Associates, Inc., Las Vegas, NV.

### REFERENCES CITED

- Bennett, R. J.; Beyand, W. R.; and Hurlbert, M. H., 1991, Microstructure of fine-grained sediments, from mud to shale: Berlin, Springer-Verlag, 582 p.
- Boggs, S., Jr., 1992, Petrology of Sedimentary Rocks: New York, MacMillan, 707 p.
- Claassen, J. C., 1986, Late-Wisconsin paleohydrology of the west-central Amargosa Desert, Nevada, USA: Chem. Geol. (Isotope Geosci. Sect.), v. 58, p. 311–323.
- Dorne, R. I., 1988, A rock varnish interpretation of alluvial-fan development in Death Valley, California: Nat. Geog. Res., v. 4, p. 56–73.
- \_\_\_\_\_, 1989, A comment on 'A note on the characteristics and possible origins of desert varnishes from southeast Morocco' by Drs. Smith and Whalley: Earth Surf. Proc. Landforms, v. 14, p. 167–170.
- \_\_\_\_\_, 1990, Quaternary alkalinity fluctuations recorded in rock varnish microlaminations on western USA volcanics: Palaeogeog. Palaeoclimat. Palaeocol., v. 76, p. 291–310.
- \_\_\_\_\_, 1994, Rock varnish as evidence of climatic change, in Abrahams, A. D., and Parsons, A. J., eds., Geomorphology of Desert Environments: London, Chapman & Hall, p. 539–552.
- \_\_\_\_\_, and DeNiro, M. J., 1985, Stable carbon isotope ratios of rock varnish organic matter: a new paleoenvironmental indicator: Science, v. 227, p. 1472–1474.
- \_\_\_\_\_, Jull, A. J. T.; Donahue, D. J.; Linick, T. W.; and Toolin, L. J., 1989, Accelerator mass spectrometry radiocarbon dating of rock varnish: Geol. Soc. America Bull., v. 101, p. 1363–1372.
- \_\_\_\_\_, and Krinsley, D. H., 1991, Cation-leaching sites in rock varnish: Geology, v. 19, p. 1077–1080.
- \_\_\_\_\_, \_\_\_\_\_; Liu, T.; Anderson, S.; Clark, J.; Cahill, T. A.; and Gill, T. E., 1992, Manganese-rich rock varnish does occur in Antarctica: Chem. Geol. v. 99, p. 289–298.
- \_\_\_\_\_, and Meek, N., 1995, Rapid formation of rock varnish and other rock coatings on slag deposits near Fontana, California: Earth Surf. Proc. Landforms, v. 20, in press.
- \_\_\_\_\_, and Oberlander, T. M., 1981, Microbial origin of desert varnish: Science, v. 213, p. 1245–1247.
- \_\_\_\_\_, and \_\_\_\_\_, 1982, Rock varnish: Progress in Physical Geography, v. 6, p. 317–367.
- Dragovich, D., 1988, Desert varnish and environmental change near Broken Hill, western New South Wales: Earth Sci. Rev., v. 25, p. 399–407.
- \_\_\_\_\_, 1993, Distribution and chemical composition of microcolonial fungi and rock coatings from arid Australia: Phys. Geog., v. 4, p. 323–341.
- Drake, N.A.; Heydeman, M.T.; and White, K. H., 1993, Distribution and formation of rock varnish in southern Tunisia: Earth Surf. Proc. Landforms, v. 18, p. 31–41.
- Douglas, G. R., 1987, Manganese-rich rock coatings from Iceland: Earth Surf. Proc. Landforms, v. 12, p. 301–310.
- El-Demerdashe, S.; El-Dadi, H. A.; Foda, M. S.; and Abdel-Hamid, E. A., 1982, Desorption of manganese retained by clay minerals: Egypt Jour. Soil Science, v. 22, p. 2138–218.
- Ferris, F. G.; Fyfe, W. S.; and Beveridge, T. J., 1987, Manganese oxide deposition in a hot spring microbial mat.: Geomicrobiology Journal, v. 5, p. 33–42.

- Forcada, M. K., and Mate, C. M., 1993, Molecular layering during evaporation of ultrathin liquid films: *Nature*, v. 363, p. 527–529.
- Friedmann, E. I., ed., 1993, *Antarctic Microbiology*, New York, Wiley, 634 p.
- Haberland, W., 1975, Untersuchungen an Krusten, Wustenlacken und Polituren auf Gesteinsoberflächen der nordlichen und mittleren Saharan (Libyen und Tschad): *Berliner Geographische Abhandlungen*, v. 21, p. 1–77.
- Hobbs, W. H., 1917, The erosional and degradational processes of deserts, with especial reference to the origin of desert depressions: *Annals Assoc. Am. Geog.*, v. 7, p. 25–60.
- Hooke, R. L., 1972, Geomorphic evidence for late Wisconsin and Holocene tectonic deformation, Death Valley, California: *Geol. Soc. America Bull.*, v. 83, p. 2073–2098.
- , Yang, H., and Weiblen, P. W., 1969, Desert varnish: an electron probe study: *Jour. Geology*, v. 77, p. 275–288.
- Jones, C. E., 1991, Characteristics and origin of rock varnish from the hyperarid coastal deserts of northern Peru: *Quat. Res.*, v. 35, p. 116–129.
- Krinsley, D., and Dorn, R. I., 1991, New eyes on eastern California rock varnish: *California Geology*, v. 44 (5), p. 107–115.
- ; ———; and Anderson, S., 1990, Factors that may interfere with the dating of rock varnish: *Phys. Geog.*, v. 11, p. 97–119.
- ; Nagy, B.; Dypvik, H.; and Rigali, M., 1993, Microtextures in mudrocks as revealed by backscattered electron imaging: *Precamb. Res.*, v. 61, p. 191–207.
- Krumbein, W. E., and Jens, J., 1981, Biogenic rock varnishes of the Negev Desert (Israel): an ecological study of iron and manganese transformation by cyanobacteria and fungi: *Oecologia*, v. 50, p. 25–38.
- McLaren, A. C., 1991, *Transmission electron microscopy of minerals and rocks*: Cambridge, Cambridge University Press, 387 p.
- Nagy, B.; Nagy, L. A.; Rigali, M. J.; Jones, W. D.; Krinsley, D. H.; and Sinclair, N., 1991, Rock varnish in the Sonoran Desert: microbiologically mediated accumulation of manganese in sediments: *Sedimentology*, v. 38, p. 1153–1171.
- Palmer, F. E.; Staley, J. T.; Murray, R. G. E.; Counsell, T.; and Adams, J. B., 1985, Identification of manganese-oxidizing bacteria from desert varnish: *Geomicrobiology Journal*, v. 4, p. 343–360.
- Perry, R. S., and Adam, J., 1978, Desert varnish: evidence of cyclic deposition of manganese: *Nature*, v. 276, p. 489–491.
- Potter, R. M., and Rossmann, G. R., 1977, Desert varnish: the importance of clay minerals: *Science*, v. 196, p. 1446–1448.
- , and ———, 1979, The manganese- and iron-oxide mineralogy of desert varnish: *Chem. Geol.*, v. 25, p. 79–94.
- Raymond, R. J.; Guthrie, G. D. J.; Bish, D. L.; Reneau, S. L.; and Chipera, S. J., 1992, Biomineralization of manganese within rock varnish: *Catena Suppl.*, v. 21, p. 321–335.
- Robert, M., and Tessier, D., 1992, Incipient weathering: some new concepts on weathering, clay formation, and organization, in Martini, I. P., and Chesworth, W., eds., *Weathering, Soils, and Paleosols*: Amsterdam, Elsevier, p. 71–105.
- Smith, B. J., and Whalley, W. B., 1988, A note on the characteristics and possible origins of desert varnishes from southeast Morocco: *Earth Surf. Proc. Landforms*, v. 13, p. 251–258.
- Staley, J. T.; Adams, J. B.; and Palmer, F. E., 1991, Desert varnish: a biological perspective: *Soil Biochem.*, v. 7, p. 173–195.
- Stumm, W., and Morgan, J. J., 1981, *Aquatic Chemistry* (2d ed.): New York, Wiley, 780 p.
- Uren, N. C., and Leeper, G. W., 1978, Microbial oxidation of divalent manganese: *Soil Biology and Biochemistry*, v. 10, p. 85–87.
- Wells, P. V., and Woodcock, D., 1985, Full-glacial vegetation of Death Valley, California. Juniper woodland opening to *Yucca* semidesert: *Madrono*, v. 32, p. 11–23.